NUCL SCI TECH (2020) 31:117
https://doi.org/10.1007/s41365-020-00825-3

BL19U2: Small-angle X-ray scattering beamline for biological macromolecules in solution at SSRF

Yi-Wen Li[1] · Guang-Feng Liu[1] · Hong-Jin Wu[1,2] · Ping Zhou[1] · Chun-Xia Hong[1] · Na Li[1] · Feng-Gang Bian[1,3]

Received: 19 September 2020 / Revised: 26 October 2020 / Accepted: 30 October 2020 / Published online: 4 December 2020

Abstract The BL19U2 at the Shanghai Synchrotron Radiation Facility is a small-angle X-ray scattering beamline dedicated to structural studies pertaining to biological macromolecules in solution. The beamline has been officially opened to users in March 2015, and since then, a series of technological innovations has been developed to optimize beamline performance, thereby significantly improving the data collection efficiency and broadening the application scope of biological small-angle X-ray scattering. BL19U2 is ideal for the high-throughput screening of weakly scattered proteins, protein assemblies, nucleic acids, inorganic nanomaterials, and organic drug molecules. This paper describes the design and overview of the BL19U2 beamline. Versatile sample environments at the experimental station and some recent scientific highlights are presented.

This work was supported by the National Natural Science Foundation of China (Nos. U1832215 and U1832144) and the Youth Innovation Promotion Association of Chinese Academy Science (No.2017319).

✉ Na Li
lina02@sari.ac.cn

✉ Feng-Gang Bian
bianfg@sari.ac.cn

[1] Shanghai Advanced Research Institute (Zhangjiang Laboratory), Chinese Academy of Sciences, Shanghai 201204, China

[2] CAS Key Laboratory of Molecular Virology and Immunology, Institute Pasteur of Shanghai, Chinese Academy of Sciences, Shanghai 200031, China

[3] University of Chinese Academy of Sciences, Beijing 100049, China

Keywords Shanghai synchrotron radiation facility · Biological small-angle X-ray scattering · High-throughput screening · Biological macromolecules

1 Introduction

Small-angle X-ray scattering (SAXS) on biological macromolecules in solution is a powerful and typically used technique in molecular and structural biology; it complements crystallography, nuclear magnetic resonance spectroscopy, and other structural methods [1-2]. Modern applications of biological small-angle X-ray scattering (BioSAXS) include low-resolution shape modeling, characterization of multidomain proteins and protein–RNA complexes, and investigations of protein structural dynamic processes [3-4]. The trend toward more challenging systems, such as intrinsically disordered proteins (IDPs) and membrane proteins, is likely to continue owing to anticipated technology breakthroughs in both software and hardware. The increasing popularity of solution SAXS is associated with the construction of modern dedicated BioSAXS synchrotron beamlines worldwide [5-8], including the BL19U2 located at the Shanghai Synchrotron Radiation Facility (SSRF).

As a dedicated BioSAXS beamline, BL19U2 has been engineered to offer a high brilliance X-ray beam for time-resolved and kinetic scattering experiments; furthermore, it can optimize the collection of weak scattering signals from biological macromolecules in solution [9]. Owing to the increasing demand for BioSAXS measurements, a series of upgrades has been performed at BL19U2, including optics components, sample environments, and data-acquisition systems [10]. Consequently, the stability of the beamline

improved, thereby enabling reliable scattering data collection.

Since the last upgrade, user turnover has increased further. Currently, BL19U2 serves more than 80 user groups per year, mainly from the structural biology community. Herein, we provide a brief introduction of the design and overall technical properties of BL19U2. The versatile experimental setups used at the BL19U2 end-station are described as well. Finally, we review some SAXS applications for biological macromolecules in solution with data support from BL19U2. The purpose of this study is to provide guidance to potential users of the BioSAXS beamline.

2 Beamline overview

BL19U2 is characterized by a focused monochromatic X-ray beam from an undulator source, which shares one straight section with protein complex crystallographic beamline BL19U1 [11]. The two small-gap in-vacuum U20 undulators of BL19U1 and BL19U2 are canted by 6 mrad to provide sufficient horizontal beam separation and prevent mutual interference in the flux. A Si(111) double-crystal monochromator is used for X-ray monochromatization within 7–15 keV, and a pair of horizontal (H) and vertical (V) focusing mirrors are used to focus the beam size to 0.33 mm (H) × 0.05 mm (V) (FWHM) at the detector plane (Fig. 1). A collimated flux of $\sim 10^{12}$ photons s^{-1} at 12 keV can be introduced regularly to the beamline experimental hutch.

The vacuum tube in the experimental hutch was designed for variable length from 0.5 m to 7 m (usually set as 2.6 m), which allows the adjustable sample-to-detector distance to meet the characteristic length requirements of measured samples. Two sets of slits are mounted in vacuum in front of the sample to eliminate parasitic scattering. To further reduce the parasitic scattering of the last slits that contribute to background scattering, particularly at low angles, in-house-modified scatterless slits are installed at BL19U2 for an accurate subtraction of background scattering [10]. An in-house-developed miniature 3 mm active beamstop is mounted in the vacuum tube in front of the detector to monitor the beam intensity and transmission during data collection [10].

2.1 SAXS and WAXS configuration

Extending the scattering vector q ($q = 4\pi\sin\theta/\lambda$, where λ is the wavelength and 2θ the scattering angle) from small-angle to wide-angle regions can provide structural information with higher spatial resolutions [12]. The scattering data of SAXS and wide-angle X-ray scattering (WAXS) can be obtained simultaneously at BL19U2 (-Figs. 2 and 3). A Pilatus 1 M detector, which is mounted on railings for position adjustment, is used for SAXS data acquisition. Meanwhile, a Pilatus 300 K detector, which is installed off-axis above the direct beam, is used as the WAXS detector. It is positioned on a support holder and can be rotated and moved both vertically and horizontally to increase the accessible WAXS measurement range. In principle, the scattering intensity in the WAXS range is typically weaker than that in the SAXS range, and the scattering from the buffer and sample chamber is more considerable in wide angles [12]. Therefore, the undesired air background must be reduced. To improve the data quality, the vacuum pipe between the sample and detectors of BL19U2 was optimized to minimize the unnecessary air gap. Together with the adjustments of detector offset position, sample-to-detector distance and X-ray wavelength, the accessible scattering vector q can cover a wide range. If required, the q ranges can overlap in simultaneous SAXS and WAXS measurements. For example, in an usual instrument layout for solution scattering, the SAXS detector can be set at the position of 2.6 m from the sample at an X-ray energy of 12 keV ($\lambda = 1.03$ Å), and the WAXS detector can be positioned above the sample to collect X-ray scattered between 3.2° and 15°. With an overlap of accessible scattering angles, the data are recorded in the range q = 0.007–1.6 $Å^{-1}$, corresponding to a real space resolution of 0.4–80 nm.

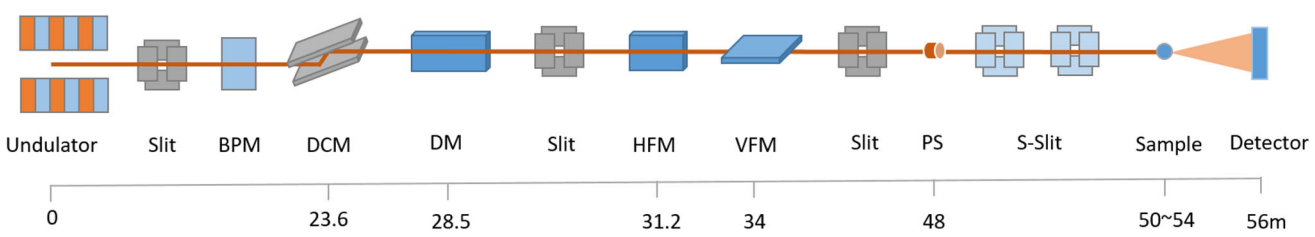

Fig. 1 (Color online) Layout of BL19U2 beamline with source-to-main element distances. Abbreviations: beam-position monitor (BPM), double-crystal monochromator (DCM), deflection mirror (DM), horizontally focusing mirror (HFM), vertically focusing mirror (VFM), photon shutter (PS), scatterless slit (S-Slit)

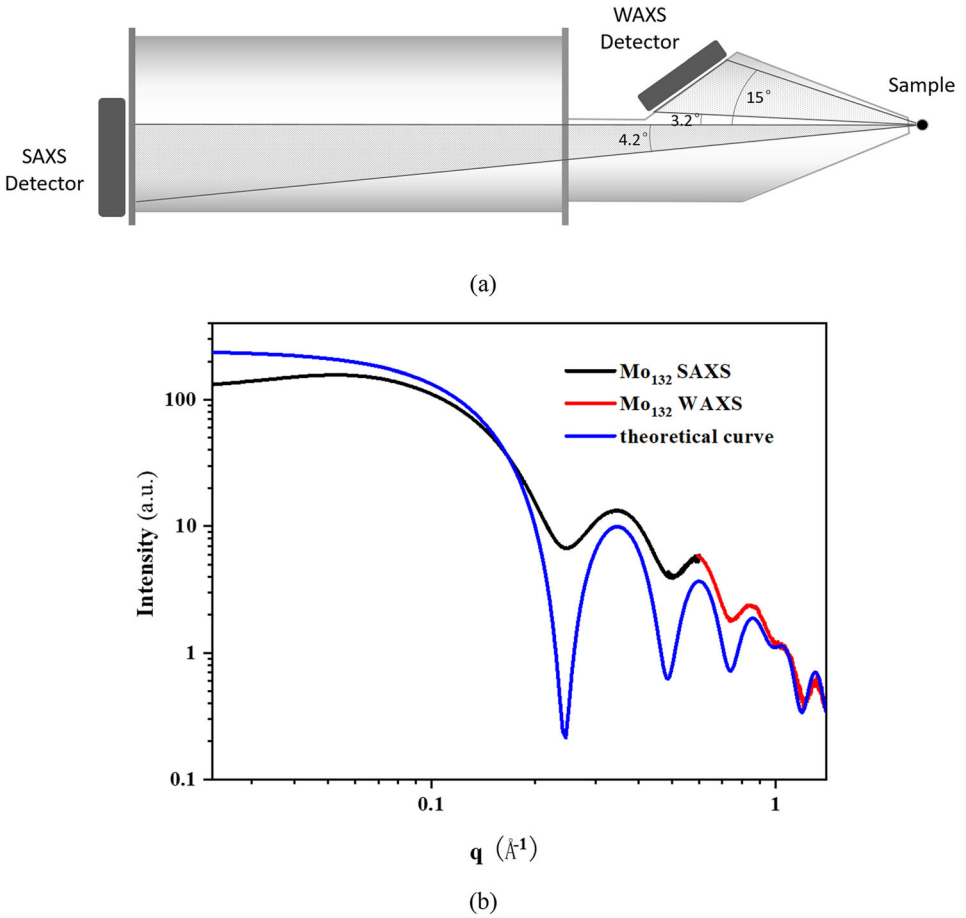

Fig. 2 (Color online) **a** Layout for solution scattering in simultaneous SAXS and WAXS measurements. **b** Full SAXS and WAXS scattering curves of nanoscale cluster Mo_{132} and theoretical curve generated from crystal structure [13]

2.2 Beamline control

The control system of BL19U2 was developed in-house [9, 14, 15] based on the EPICS (Experimental Physics and Industrial Control System) platform for the overall beamline device communication. The simultaneous operation of SAXS and WAXS detectors is integrated into the control system. Data collection is initiated by triggering the detector device servers, opening the shutter and recording the transmitted intensity for single or multiple exposures. In addition, the control software for our versatile experimental setups (Sects. 3.2–3.4) is integrated into the EPICS control platform. The user-friendly experimental control panels simplify user operations with automated sample loading and data collection. Details of the BL19U2 control system have been described elsewhere [9, 10, 14, 16].

3 BioSAXS measurements at BL19U2

BL19U2 is a high-throughput beamline dedicated to biological macromolecules in solution. It facilitates experiments performed by biochemists and structural biologists with high automation. This section outlines the experimental setups and ancillary facilities at BL19U2. The general procedures for sample preparation and data analysis are discussed as well. For the theoretical basis and technical details of BioSAXS, readers can refer to other excellent reviews and protocols [17–19].

3.1 Sample preparation

The sample preparation for BioSAXS measurements is similar to the methods used for other experimental biophysical techniques. The purity and size monodispersity of the measured samples ensure the interpretability and high-quality of scattering data. Scattering signals from undesirable aggregates, oligomers or impurities can significantly alter the scattering of molecules of interest. Hence, the homogeneity of the sample should be characterized using other techniques (e.g., SDS-PAGE, dynamic light scattering, size-exclusion chromatography, analytical ultracentrifugation, etc.) before SAXS measurement.

A typical solution for BioSAXS measurement typically comprises the data collection of sample and corresponding exactly matched buffer. Imprecise buffer matching will

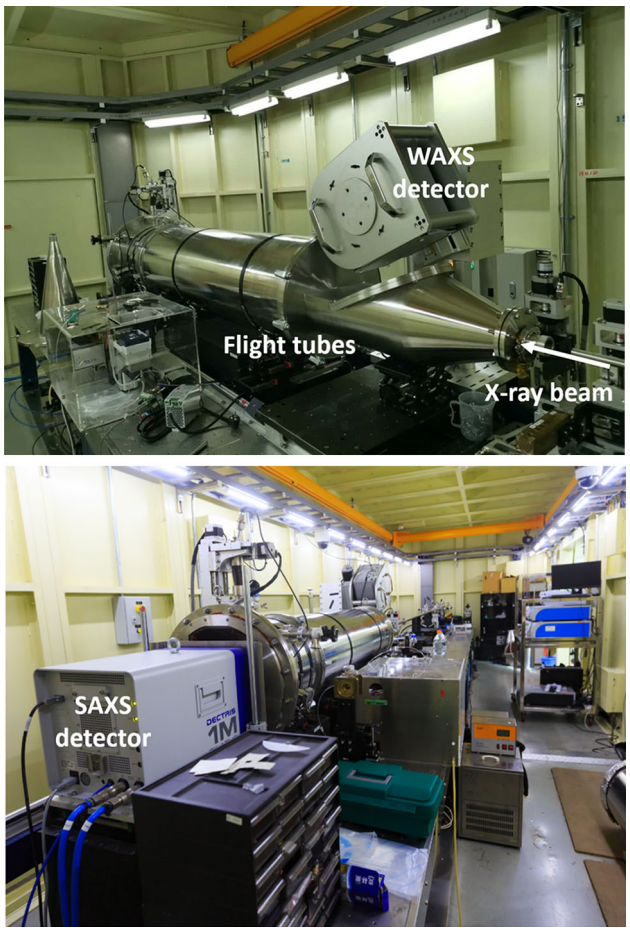

Fig. 3 (Color online) Photographs of BL19U2 experimental hutch

hinder background subtraction and structural parameter analysis. A dialysis step is recommended to ensure exact sample/buffer matching. Components of the buffer should be optimized to ensure the stability and homogeneity of the samples. The addition of salt and glycerol can reduce interparticle effects and alleviate radiation damage. However, the components added to the buffer can decrease the slight difference in electron density between the protein ($\sim$ 0.43 electrons/Å^3) and water ($\sim$ 0.33 electrons/Å^3). It is noteworthy that high-salt, glycerol, sucrose, etc., will significantly reduce the net scattering density from macromolecules. Users should be cognizant of this fact when selecting additives for the buffer.

At BL19U2, the typical sample volume required for tests using an automated sample changer is 60 µl with a concentration range from 1 to 10 mg/ml. Furthermore, a series of varied sample concentrations (3–5) can be prepared to detect and eliminate concentration-dependent effects on sample scattering. In addition, it is strongly recommended to prepare protein standards to evaluate the status of beamline setups at the beginning of the experiment. The scattering data of standard proteins can also be used to calculate the molecular weights of samples for each batch measurement. Lysozyme from hen egg white is typically used as a protein standard, which is available at BL19U2 on request.

BL19U2 is equipped with a wet laboratory on site, which comprises the most typically used laboratory devices, reagents, and consumables. Those devices include a tabletop centrifuge, a nanodrop spectrophotometer, an ultrasonic bath, a dynamic light scattering instrument, and other typical instruments (e.g., refrigerators, ultrapure water purifiers, pH meters, balances, and pipettes). They can be used freely for sample preparation and characterization before SAXS measurements.

3.2 In-air and in-vacuum automated sample changers

The dedicated sample environment is required for biological solution SAXS measurements. BL19U2 is equipped with an in-air temperature-controlled automated sample changer, which has been in commission since 2015. For more details regarding this in-air automated sample loading system, please refer to Hong et al. and Li et al. [9, 16]. Typically, samples with a volume of 60 µl are delivered to a quartz capillary and oscillated during exposure. The oscillation can significantly reduce the effects of X-ray radiation damage.

To eliminate unnecessary background scattering from air, an in-vacuum automated sample loading system was developed and successfully implemented at BL19U2 (Fig. 4a). The upgraded vacuum sample environment can significantly decrease air absorption and improve the signal-to-noise ratio of the scattering data. A detailed description of this setup and its integration into the beamline has been reported by Liu et al. [10]. Users can access both automated sample changers upon request. More information can be obtained from the beamline staff.

3.3 Inline sample purification system

The requirement for sample homogeneity is high for BioSAXS. Biological macromolecules, particularly macromolecular complexes, may potentially oligomerize or aggregate and consequently complicate scattering data analysis. To complement the standard SAXS mode, we combined an inline sample purification device with SAXS at BL19U2 by integrating size-exclusion chromatography (SEC) into scattering data collection [10] (Fig. 4b). By implementing the inline sample purification system, the outlet of a chromatography column is diverted directly to the SAXS sample holder and the scattering of separated components can be collected in consistence with elution profiles. Moreover, additional detectors, including multi-

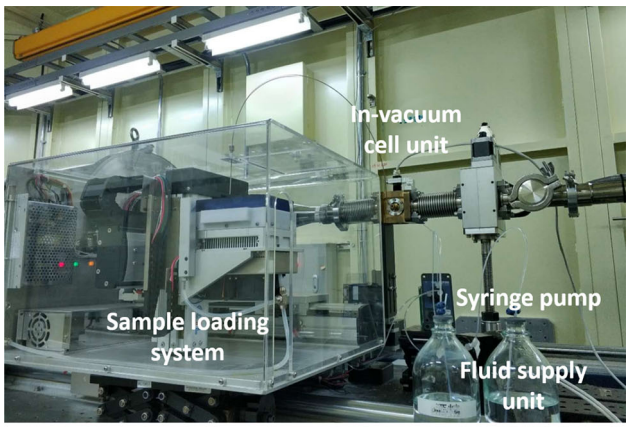

(a)

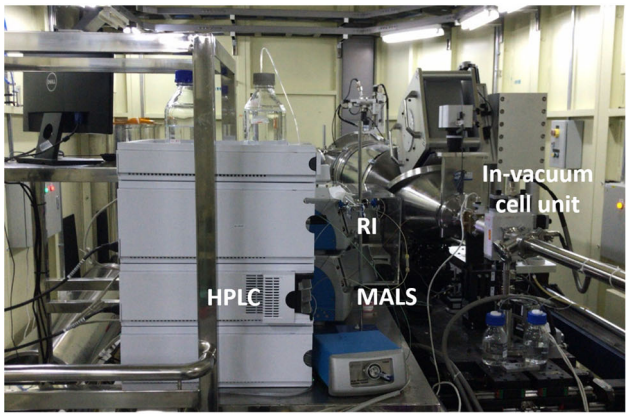

(b)

Fig. 4 (Color online) View of sample environments at BL19U2. **a** In-vacuum automated sample changer, showing in-vacuum cell unit, sample loading system, syringe pump, and fluid supply unit. **b** Inline sample purification system, showing in-vacuum cell unit, high-performance liquid chromatography (HPLC), multi-angle light scattering, and refractive index detection devices (MALS and RI)

angle light scattering, refractive index, and ultraviolet detectors, are systematically combined with SEC-SAXS for simultaneous biophysical characterization. Currently, the SEC-SAXS mode is operated stably at BL19U2. Users are encouraged to bring their own SEC columns and discuss with the beamline staff regarding their specific needs before a synchrotron visit.

3.4 Time-resolved sample environments

Time-resolved SAXS (TR-SAXS) experiments can provide valuable structural insights into complex biological processes, such as protein and RNA folding [20, 21]. Selecting an appropriate triggering mechanism for a time-resolved experiment is key for coordinating the starting point of the reaction and SAXS measurements to capture the time process of interest. Utilizing a high brilliance third-generation synchrotron source and a rapid single-photon-counting pixel detector, BL19U2 enables measurement times in the millisecond range by integrating an inline stopped-flow mixing system. In detail, an SFM2000 Biologic Stopped-flow device (Bio-Logic, France), which relies on the turbulent mixing of two fluids with a dead time of approximately 3 ms, is equipped at BL19U2. Owing to the repetition rate limit of the Pilatus 1 M SAXS detector, a time resolution of 33 ms can be probed for a kinetic reaction. It is noteworthy that the large quantity of sample consumed is a disadvantage of this stopped-flow mixing system. In general, up to several milliliters of samples are required for repeated measurements of high-quality data.

To compliment stopped-flow mixing, we recently developed continuous-flow devices to satisfy the requirement for higher time resolutions. Continuous-flow microfluidic mixing, which follows kinetics as a function of distance from the mixing point, is the most widely applicable method for initiating submillisecond reactions [22]. The basic design for the continuous-flow micromixer at BL19U2 is in reference to Ansari et al. [23]. Currently, we are testing several prototypes. To match the dimensions of the microfluidic channels, BL19U2 uses a set of beryllium compound refractive lenses (RXOPTICS, Germany) to focus the typical X-ray beam (H: 0.33 mm; V: 0.05 mm) down to a spot of diameter of $\sim$ 0.02 mm. This can further increase the temporal resolution along the observation channel of the microfluidic device.

In principle, the kinetic reaction can be triggered in different ways. In addition to the stopped-flow and microfluidic mixing described above, several mechanisms have been reported, including temperature- and pressure-jump methods. The BL19U2 staff are experienced in the design of high-pressure X-ray cells and temperature-jump microfluidic devices [24]. Users are encouraged to discuss with the beamline staff regarding their specific kinetic reaction requirements; furthermore, users are encouraged to furnish their own customized sample devices.

3.5 Data analysis and remote control

Consistent with the full automation of SAXS measurements at BL19U2, we recently deployed an automated SAXS data processing pipeline (*SAS-cam*) and installed a beta version on the beamline [25]. Beginning from handling two-dimensional scattering patterns and ending with building low-resolution three-dimensional (3D) models, the *SAS-cam* program was implemented to cope with large data volumes in a high-throughput experiment. Users can access the analyzed datasets by visiting the output via web browser. The analyzed structure parameters, including the maximum dimension D_{max}, radius of gyration R_g, estimated molecular mass and a low-resolution 3D model are

tabulated. The real-time feedback results can help users evaluate the data quality and perform adjustments for subsequent SAXS measurements. In addition, other SAXS data processing software packages, such as *BioXTAS RAW* [26] and *ATSAS* [27] are available on the beamline.

BL19U2 offers remote control for geographically distant users [10]. This remote control system is based on virtual private network technology. Remote users can log into the system via a web browser and then visit the GUI of the automated sample changers at BL19U2. Subsequently, they can operate the on-site devices, collect and download data at their local sites. Users who are interested in the remote control experiment mode can contact the beamline staff and request for a beamtime. Upon approval, applicants can mail their samples to the SSRF and register an account to log in at the scheduled beamtime.

3.6 Facility access

Researchers can request for a beamtime by visiting the Chinese Academy of Sciences, Sharing Service Platform of CAS Large Research Infrastructure website (http://lssf.cas.cn/). The BL19U2 beamline is listed in the facility catalog of the National Facility for Protein Science Shanghai (NFPSS). Potential users should consult the beamline staff to discuss the feasibility of measurements.

4 Scientific highlights

Since 2015, BL19U2 has served more than 180 user groups and has been productive during the past five years. The numerous data collected at BL19U2 facilitated the publication of many cutting-edge scientific research papers. In the sections below, we review some recent publications that may aid potential BioSAXS users to understand the effectiveness of this technique for the structural characterization of biological macromolecules.

4.1 Structure validation and refinement

As a complementary technique in structural biology, the most straightforward application of SAXS is for structure validation and refinement. An example is the structural studies of the *Staphylococcus aureus* response regulator ArlR—a key two-component regulatory system necessary for adhesion and biofilm formation [28]. The response regulator ArlR comprises an N-terminal receiver domain and a C-terminal DNA-binding effector domain. Yurong Wen's group solved the crystal structure of the ArlR effector domain and discovered that the effector domain crystallized as a domain-swapped dimer. To validate the ArlR DNA-binding domain structure, researchers performed SAXS experiments at BL19U2. The overall comparison of SAXS experimental data to the crystal structure of the ArlR DNA-binding domain further confirmed that the $\beta1$-$\beta2$ hairpin was dissociated from the rest of the domain, indicating the formation of a non-canonical $\beta1$-$\beta2$ hairpin domain swapping (Fig. 5).

In addition to X-ray crystallography, NMR is another frequently used method for protein structure characterization. SAXS can provide long-distance restraints to increase the accuracy of protein structure determination via NMR. In a case pertaining to the zinc finger domain of METTL3 (METTL3 ZFD), Chun Tang's group performed SAXS experiments and applied distance distribution restraints derived from SAXS data during the structural characterization of METTL3 ZFD using NMR [29].

4.2 Modeling multidomain proteins and complex particles

The reconstruction of a relatively low-resolution molecule envelope from scattering data is one of the major

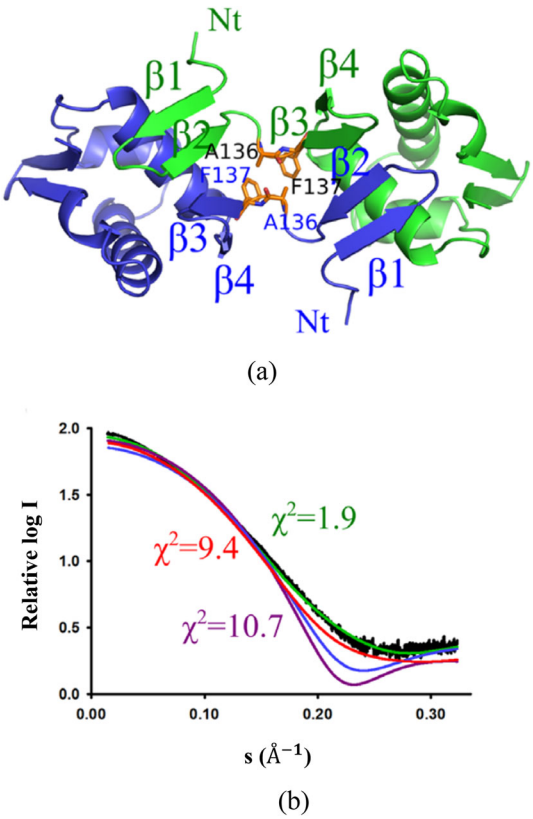

Fig. 5 (Color online) Structure of ArlR DNA-binding domain. **a** ArlR DNA-binding domain dimer generated from a symmetrical unit cell. **b** ArlR DNA-binding domain SAXS experimental curve (black) fitted to curves generated from the crystal structure (green), demonstrating a strong correlation between the crystal and solution structures of ArlR DNA-binding domain [28]

advances in SAXS. Furthermore, SAXS is particularly informative if one subdomain of the complex undergoes a conformational change upon binding. Changrui Lu's group presented the structure model of a ribonucleoprotein complex of prohead RNA (pRNA) and gene product 16 (gp16) ATPase as well as their conformation change in response to ATP or ADP binding [30]. Considering the self-assembly nature and base complementarity in the pRNA domain, SEC-SAXS experiments were performed to ensure sample monodispersity. By combining ab initio and rigid-body modeling, the researchers confirmed the relative positions of pRNA and gp16. To visualize the multiple conformations of the pRNA-gp16 complex induced by ATP and ADP, the respective molecular bead model was calculated from the SAXS profiles. The models indicated that the entire complex closed in the presence of ATP, whereas pRNA domain II rotated and opened as ATP hydrolyzed (Fig. 6).

Another example is the structural studies of RNA helicase DDX21, which is critical to the regulation of host innate immunity during virus infection [31]. Jixi Li's group investigated different solution states of DDX21 using the SAXS method to further clarify the conformational change in DDX21 upon binding with RNA. The SAXS patterns of three DDX21 molecules were recorded to generate the final composite scattering curves. Further superimposing SAXS ab initio envelopes with their crystal structures yielded an excellent fitting, revealing an open to closed conformational change upon RNA binding and unwinding.

4.3 Flexible systems

Combined with suitable computational methods, SAXS can provide potentially unrestricted access to the conformational spaces of flexible systems, a clear advantage over traditional techniques such as crystallography. An excellent example of a flexible system investigated via SAXS is long non-coding subgenomic flavivirus RNAs (sfRNA), which are critical to pathogenicity and immune evasion [32]. Xianyang Fang's group studied the 3D structures of individual and combined subdomains of sfRNA. Computational modeling and the ensemble optimization method (EOM) were used to characterize the structural ensembles of complete sfRNAs against SAXS data. The EOM generated multiple conformers, followed by selections based on their compatibility with the experimental SAXS data. It was demonstrated that SAXS is an ideal tool for investigating the conformational spaces of flexible systems in solution (Fig. 7).

Moreover, SAXS is suitable for studying IDPs, which are either disordered or contain long stretches of unstructured regions. Owing to the lack of rigid, well-defined structures, the characterization of IDPs is challenging for structural biologists. However, IDPs or flexible proteins can be characterized by global features derived from SAXS data, such as the Kratky plot or pair-distribution function. Yang Sun's group used SAXS combined with multiple experimental methods to investigate the structure of caseinate particles, which are typical IDPs [33]. The SREFLEX program for normal mode analysis was used in that study to estimate the flexibility of models by fitting the SAXS profile of caseinate with assemblies.

5 Concluding remarks

Characterized by high brilliance and full automation, the BioSAXS beamline BL19U2 is primarily designed for solution-scattering measurements. Meanwhile, the upgraded BL19U2 can perform high-throughput data collection in a completely automated manner. Simultaneous SAXS and WAXS measurements can offer more information with a broader scattering vector range. The dedicated and versatile sample environments at BL19U2 provide more alternatives for user experiments that involve specific requirements. For example, in-air and in-vacuum automated sample changers can provide optimum conditions for solution SAXS, enabling high-throughput studies. Meanwhile, the inline sample purification system and time-resolved experimental setups enable the analysis of more

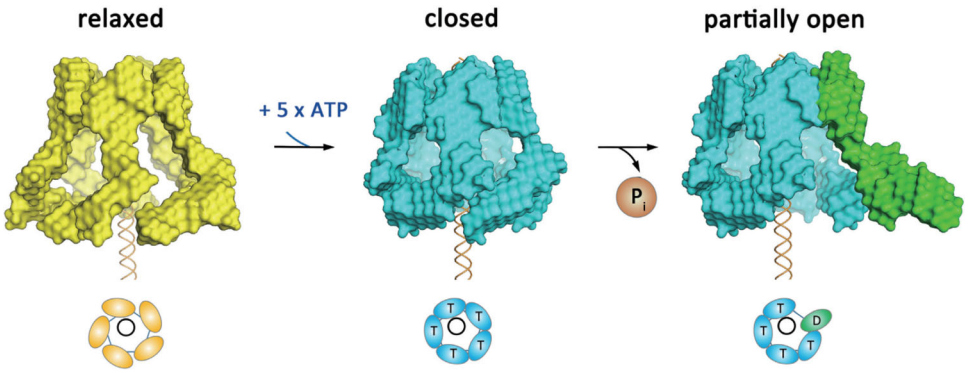

Fig. 6 (Color online) Reconstructed 3D models of phi29 molecular movement during ATP binding and hydrolysis [30]

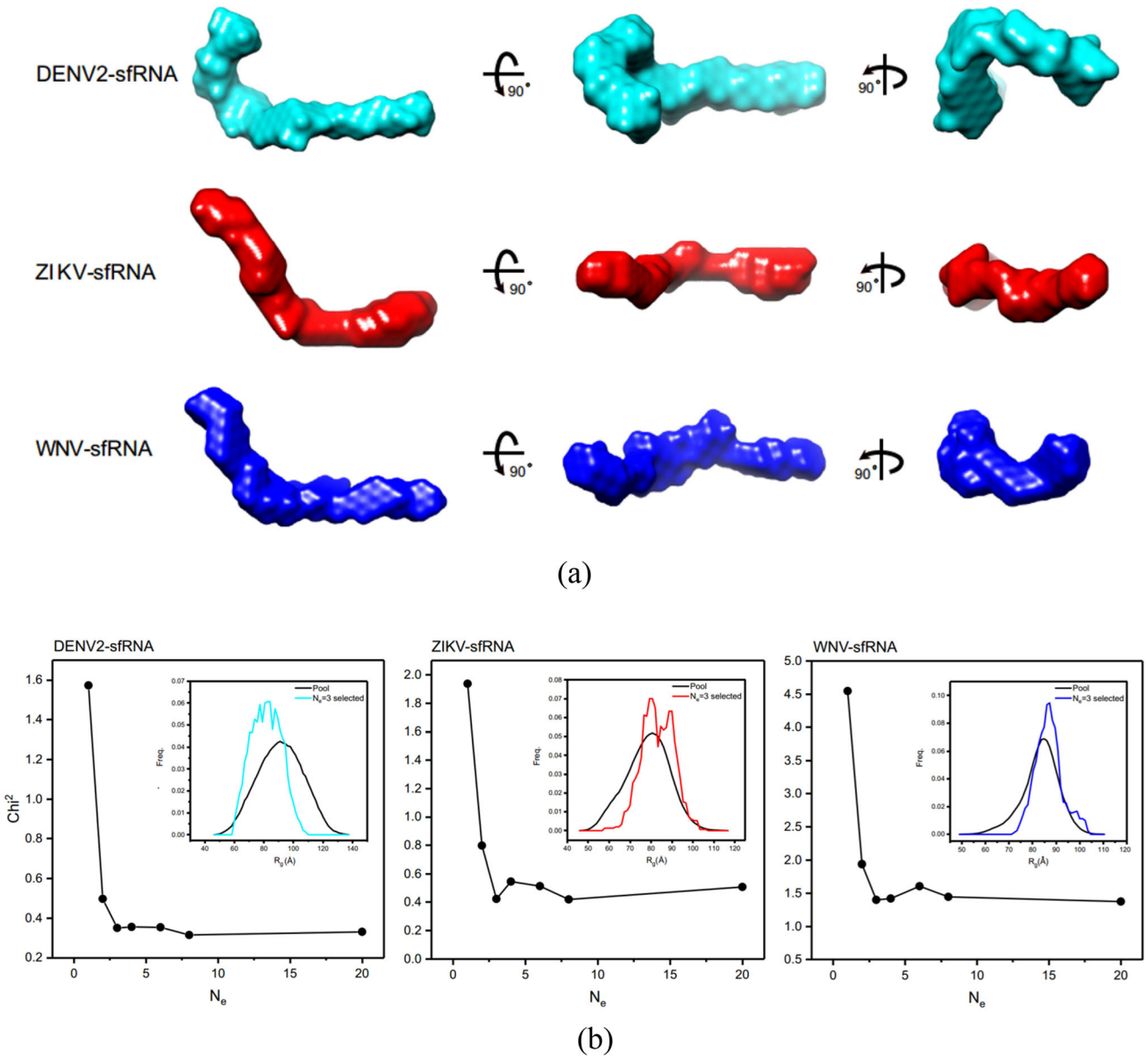

Fig. 7 (Color online) Structural analysis of complete sfRNAs via SAXS. **a** Ab initio shape envelopes of complete sfRNAs. **b** Fitted chi-square plotted against ensemble size for complete sfRNAs [32]

complicated systems and the tracing of dynamic processes. Moreover, the automated SAXS data processing pipeline, *SAS-cam*, allows for real-time evaluations, and users can promptly adjust their experimental plan based on feedback results.

Future work at BL19U2 will focus on enhancing its capacity for dedicated BioSAXS measurements. Small sample volume with ultra-dilute concentration is a prospective requirement, which can be satisfied by developing applicable microfluidic devices. A second-generation in-vacuum automated sample loading system, which can be operated more reliably with lower sample volume consumption, is currently being developed at BL19U2. A high-pressure sample chamber is being prepared to enrich the existing versatile sample environments. Benefiting from the construction of the integrated structural biology platform at the NFPSS, we are investigating an X-ray footprinting device that can be used to observe the structure and dynamics of biological macromolecules by studying their interactions in the native solution state.

Acknowledgements The authors thank the SSRF Small-Angle Scattering Group at BL16B for operation and technical support. Additionally, we thank Prof. Pan-Chao Yin (South China University of Technology) for providing samples and theoretical scattering data of the nanoscale cluster Mo_{132}.

References

1. M.H.J. Koch, P. Vachette, D.I. Svergun, Small-angle scattering: a view on the properties, structures and structural changes of biological macromolecules in solution. Q. Rev. Biophys. **36**(2), 147–227 (2003). https://doi.org/10.1017/S0033583503003871
2. M.A. Graewert, D.I. Svergun, Impact and progress in small and wide angle X-ray scattering (SAXS and WAXS). Curr. Opin. Struct. Biol. **23**(5), 748–754 (2013). https://doi.org/10.1016/j.sbi.2013.06.007
3. J. Lipfert, S. Doniach, Small-angle X-ray scattering from RNA, proteins, and protein complexes. Annu. Rev. Biophys. Biomol. Struct. **36**, 307–327 (2007). https://doi.org/10.1146/annurev.biophys.36.040306.132655
4. B.N. Chaudhuri, Emerging applications of small angle solution scattering in structural biology. Protein Sci. **24**(3), 267–276 (2015). https://doi.org/10.1002/pro.2624
5. I.L. Smolsky, P. Liu, M. Niebuhr et al., Biological small-angle x-ray scattering facility at the Stanford synchrotron radiation laboratory. J. Appl. Cryst. **40**, s453–s458 (2007). https://doi.org/10.1107/S0021889807009624
6. P. Pernot, A. Round, R. Barrett et al., Upgraded ESRF BM29 beamline for SAXS on macromolecules in solution. J. Synchrotron Radiat. **20**, 660–664 (2013). https://doi.org/10.1107/S0909049513010431
7. A.S. Acerbo, M.J. Cook, R.E. Gillilan, Upgrade of MacCHESS facility for X-ray scattering of biological macromolecules in solution. J. Synchrotron Radiat. **22**, 180–186 (2015). https://doi.org/10.1107/S1600577514020360
8. C.E. Blanchet, A. Spilotros, F. Schwemmer et al., Versatile sample environments and automation for biological solution X-ray scattering experiments at the P12 beamline (PETRA III, DESY). J. Appl. Cryst. **48**, 431–443 (2015). https://doi.org/10.1107/S160057671500254X
9. N. Li, X.H. Li, Y.Z. Wang et al., The new NCPSS BL19U2 beamline at the SSRF for small-angle X-ray scattering from biological macromolecules in solution. J. Appl. Cryst. **49**, 1428–1432 (2016). https://doi.org/10.1107/S160057671601195X
10. G.F. Liu, Y.W. Li, H.J. Wu et al., Upgraded SSRF BL19U2 beamline for small-angle X-ray scattering of biological macromolecules in solution. J. Appl. Cryst. **51**, 1633–1640 (2018). https://doi.org/10.1107/S160057671801316X
11. W.Z. Zhang, J.C. Tang, S.S. Wang et al., The protein complex crystallography beamline (BL19U1) at the Shanghai Synchrotron Radiation Facility. Nucl. Sci. Tech. **30**(11), 170 (2019). https://doi.org/10.1007/s41365-019-0683-2
12. Y.J. Wang, H. Zhou, E. Onuk et al., What can we learn from wide-angle solution scattering? Biological small angle scattering: techniques, strategies and tips. Adv. Exp. Med. Biol. **1009**, 131–147 (2017). https://doi.org/10.1007/978-981-10-6038-0_8
13. P.C. Yin, B. Wu, T. Li et al., Reduction-triggered self-assembly of nanoscale molybdenum oxide molecular clusters. J. Am. Chem. Soc. **138**(33), 10623–10629 (2016). https://doi.org/10.1021/jacs.6b05882
14. P. Zhou, C.X. Hong, Y.Z. Wang et al., The control system and the data acquisition system of biological small angle ray scattering beamline. Nucl. Tech. **39**(9), 090101 (2016). https://doi.org/10.11889/j.0253-3219.2016.hjs.39.090101 (**in Chinese**)
15. P. Liu, Y.N. Zhou, Q.R. Mi et al., EPICS-based data acquisition system on beamlines at SSRF. Nucl. Tech. **33**, 415–419 (2010). (**in Chinese**)
16. C.X. Hong, P. Zhou, Y.W. Li et al., An automatic solution-sample-changing peristaltic device at biological small angle X-ray scattering beamline. Nucl. Tech. **39**(1), 010102 (2016). https://doi.org/10.11889/j.0253-3219.2016.hjs.39.010102 (**in Chinese**)
17. A. Grishaev, Sample preparation, data collection, and preliminary data analysis in biomolecular solution X-ray scattering. Curr. Protoc. Protein Sci. **17**, 14 (2012). https://doi.org/10.1002/0471140864.ps1714s70
18. S. Skou, R.E. Gillilan, N. Ando, Synchrotron-based small-angle X-ray scattering of proteins in solution. Nat. Protoc. **9**(7), 1727–1739 (2014). https://doi.org/10.1038/nprot.2014.116
19. C.M. Jeffries, M.A. Graewert, C.E. Blanchet et al., Preparing monodisperse macromolecular samples for successful biological small-angle X-ray and neutron-scattering experiments. Nat. Protoc. **11**(11), 2122–2153 (2016)
20. L.W. Kwok, I. Shcherbakova, J.S. Lamb et al., Concordant exploration of the kinetics of RNA folding from global and local perspectives. J. Mol. Biol. **355**(2), 282–293 (2006). https://doi.org/10.1016/j.jmb.2005.10.070
21. J. Lamb, L. Kwok, X.Y. Qiu et al., Reconstructing three-dimensional shape envelopes from time-resolved small-angle X-ray scattering data. J. Appl. Cryst. **41**, 1046–1052 (2008). https://doi.org/10.1107/S0021889808028264
22. L. Pollack, M.W. Tate, N.C. Darnton et al., Compactness of the denatured state of a fast-folding protein measured by submillisecond small-angle x-ray scattering. Proc. Natl. Acad. Sci. **96**(18), 10115–10117 (1999). https://doi.org/10.1073/pnas.96.18.10115
23. M.A. Ansari, K.Y. Kim, K. Anwar et al., A novel passive micromixer based on unbalanced splits and collisions of fluid streams. J. Micromech. Microeng. **20**(5), 055007 (2010). https://doi.org/10.1088/0960-1317/20/5/055007
24. Y.W. Li, F.G. Bian, J. Wang, A novel heating area design of temperature-jump microfluidic chip for synchrotron radiation solution X-ray scattering. Nucl. Sci. Tech. **27**(4), 92 (2016). https://doi.org/10.1007/s41365-016-0083-9
25. H.J. Wu, Y.W. Li, G.F. Liu et al., SAS-cam: a program for automatic processing and analysis of small-angle scattering data. J. Appl. Cryst. **53**, 1147–1153 (2020). https://doi.org/10.1107/S1600576720008985
26. J.B. Hopkins, R.E. Gillilan, S. Skou, BioXTAS RAW: improvements to a free open-source program for small-angle X-ray scattering data reduction and analysis. J. Appl. Cryst. **50**, 1545–1553 (2017). https://doi.org/10.1107/S1600576717011438
27. M.V. Petoukhov, D. Franke, A.V. Shkumatov et al., New developments in the ATSAS program package for small-angle scattering data analysis. J. Appl. Cryst. **45**, 342–350 (2012). https://doi.org/10.1107/S0021889812007662
28. Z.L. Ouyang, F. Zheng, J.Y. Chew et al., Deciphering the activation and recognition mechanisms of Staphylococcus aureus response regulator ArlR. Nucleic Acids Res. **47**(21), 11418–11429 (2019). https://doi.org/10.1093/nar/gkz891
29. J.B. Huang, X. Dong, Z. Gong et al., Solution structure of the RNA recognition domain of METLL3-METTL14 N^6-methyladenosine methyltransferase. Protein Cell **10**(4), 272–284 (2019). https://doi.org/10.1007/s13238-018-0518-7
30. R.J. Cai, I.R. Price, F. Ding et al., ATP/ADP modulates gp16–pRNA conformational change in the Phi29 DNA packaging motor. Nucleic Acids Res. **47**(18), 9818–9828 (2019). https://doi.org/10.1093/nar/gkz692
31. Z.J. Chen, Z.Y. Li, X.J. Hu et al., Structural basis of human helicase DDX21 in RNA binding, unwinding, and antiviral signal activation. Adv. Sci. **7**(14), 2000532 (2020). https://doi.org/10.1002/advs.202000532
32. Y.P. Zhang, Y.K. Zhang, Z.Y. Liu et al., Long non-coding subgenomic flavivirus RNAs have extended 3D structures and are flexible in solution. EMBO Rep. **20**(11), e47016 (2019). https://doi.org/10.15252/embr.201847016
33. F. Gao, Y.Y. Xia, D. Chen et al., Insights on the structure of caseinate particles based on surfactants-induced dissociation. Food Hydrocoll. **104**, 105766 (2020). https://doi.org/10.1016/j.foodhyd.2020.105766